

Fast and perfect state transfer in superconducting circuit with tunable coupler

Chi Zhang(张驰), Tian-Le Wang(王天乐), Ze-An Zhao(赵泽安), Xiao-Yan Yang(杨小燕),Liang-Liang Guo(郭亮亮), Zhi-Long Jia(贾志龙), Peng Duan(段鹏), and Guo-Ping Guo(郭国平)
Citation: Chin. Phys. B, 2023, 32 (**11**): 110305. DOI: 10.1088/1674-1056/acf496
Journal homepage: http://cpb.iphy.ac.cn; http://iopscience.iop.org/cpb

What follows is a list of articles you may be interested in

High-fidelity topological quantum state transfersin a cavity-magnon system

Xi-Xi Bao(包茜茜), Gang-Feng Guo(郭刚峰), Xu Yang(杨煦), and Lei Tan(谭磊)
Chin. Phys. B, 2023, 32 (**8**): 080301. DOI: 10.1088/1674-1056/acc3f6

Engineering topological state transfer in four-period Su-Schrieffer-Heeger chain

Xi-Xi Bao(包茜茜), Gang-Feng Guo(郭刚峰), and Lei Tan(谭磊)
Chin. Phys. B, 2023, 32 (**2**): 020301. DOI: 10.1088/1674-1056/ac7bfe

Change-over switch for quantum states transfer with topological channels in a circuit-QED lattice

Liu-Yong Cheng(程留永), Li-Na Zheng(郑黎娜), Ruixiang Wu(吴瑞祥), Hong-Fu Wang(王洪福), and Shou Zhang(张寿)
Chin. Phys. B, 2022, 31 (**2**): 020305. DOI: 10.1088/1674-1056/ac2f2e

Enhancement of multiatom non-classical correlations and quantum state transfer in atom-cavity-fiber system

Qi-Liang He(贺启亮), Jian Sun(孙剑), Xiao-Shu Song(宋晓书), and Yong-Jun Xiao(肖勇军)
Chin. Phys. B, 2021, 30 (**1**): 010305. DOI: 10.1088/1674-1056/abb7f4

Fast achievement of quantum state transfer and distributed quantum entanglement by dressed states

Liang Tian(田亮), Li-Li Sun(孙立莉), Xiao-Yu Zhu(朱小瑜), Xue-Ke Song(宋学科), Lei-Lei Yan(闫磊磊), Er-Jun Liang(梁二军), Shi-Lei Su(苏石磊), Mang Feng(冯芒)
Chin. Phys. B, 2020, 29 (**5**): 050306. DOI: 10.1088/1674-1056/ab7e9a

---

RAPID COMMUNICATION

Fast and perfect state transfer in superconducting circuit with tunable coupler

Chi Zhang(张驰)[1,2,†], Tian-Le Wang(王天乐)[1,2,†], Ze-An Zhao(赵泽安)[1,2], Xiao-Yan Yang(杨小燕)[1,2], Liang-Liang Guo(郭亮亮)[1,2], Zhi-Long Jia(贾志龙)[1,2], Peng Duan(段鹏)[1,2], and Guo-Ping Guo(郭国平)[1,2,3,‡]

[1] *CAS Key Laboratory of Quantum Information, University of Science and Technology of China, Hefei* 230026, *China*
[2] *CAS Center for Excellence and Synergetic Innovation Center in Quantum Information and Quantum Physics, University of Science and Technology of China, Hefei* 230026, *China*
[3] *Origin Quantum Computing Company Limited, Hefei* 230026, *China*

(Received 1 August 2023; revised manuscript received 23 August 2023; accepted manuscript online 29 August 2023)

In quantum computation and quantum information processing, the manipulation and engineering of quantum systems to suit certain purposes are an ongoing task. One such example is quantum state transfer (QST), an essential requirement for both quantum communication and large-scale quantum computation. Here we engineer a chain of four superconducting qubits with tunable couplers to realize the perfect state transfer (PST) protocol originally proposed in quantum spin networks and successfully demonstrate the efficient transfer of an arbitrary single-qubit state from one end of the chain to the other, achieving a high fidelity of 0.986 in just 25 ns. This demonstrated QST is readily to extend to larger chain and multi-node configurations, thus serving as a desirable tool for scalable quantum information processing.

Keywords: quantum state transfer, superconducting circuit, tunable coupler

PACS: 03.67.–a, 03.67.Ac **DOI:** 10.1088/1674-1056/acf496

1. Introduction

Quantum computing has long held the promise of solving intractable problems that its classical counterpart cannot.[1,2] Superconducting quantum circuit is one of the leading candidates to build a practical quantum computer,[3] on which the experimental quantum advantage is firstly demonstrated.[4,5] Transferring information from one location to another is a fundamental requirement for both classical and quantum information processing.[6–9] High-fidelity quantum state transfer is crucial for realizing a large-scale quantum computer[10] and harnessing the full potential of contemporary state-of-the-art quantum processors.[11–14] Long-distance quantum information transfer is necessary for the communication between quantum processors, which is usually accomplished through photon-mediated[7,15,16] or phonon-mediated[17] quantum state transfer with the additional interface between stationary qubits and flying qubits. As to short-distance quantum state transfer, a key ingredient in on-chip quantum information processing, various theories have been proposed for high fidelity quantum state transfer (QST) across a stationary lattice.[8,9,18,19]

Specifically, the perfect state transfer protocol[18] (PST) realizes perfect QST across a stationary coupled lattice through Hamiltonian evolution for a fixed period of time. In an N site linear chain, the state of site n can be transferred to site $N-n+1$ perfectly with pre-engineered inter-qubit interaction. So far, PST has been experimentally demonstrated in nuclear magnetic resonance systems,[20] in optical systems with an array of coupled waveguides,[21] and in solid-state quantum systems with a chain of four superconducting transmon qubits in the fixed coupling architecture.[22] The experiment performed in the superconducting circuit relied on full control of the effective couplings between neighboring qubits by parametrically modulating the qubits. In this approach, the tunable range of the effective coupling strength is considerably limited by the intrinsic geometric coupling of the circuit, which limits its transfer speed. Moreover, due to the always-on coupling, the send-qubit and the receive-qubit can not be isolated from the chain before and after the transfer process; this will degrade its performance in a quantum network. To overcome these drawbacks, tunable coupler would be desirable in the transfer channel,[10,17] see Fig. 1(a). Recently, the tunable coupler architecture proposed by Yan Fei *et al*.[23] and its variants[24,25] have been wildly used in large-scale superconducting quantum processors. The tunable coupler is almost the same as a tunable qubit, which makes it highly compatible with state-of-the-art control and fabrication methods of superconducting circuits. The coupling strength can be tuned over approximately three orders of magnitude, and the residual ZZ interaction between neighboring qubits can also be effectively suppressed,[26] which is favorable for simultaneous quantum operations.

[†] These authors contributed equally to this work.
[‡] Corresponding author. E-mail: gpguo@ustc.edu.cn
© 2023 Chinese Physical Society and IOP Publishing Ltd

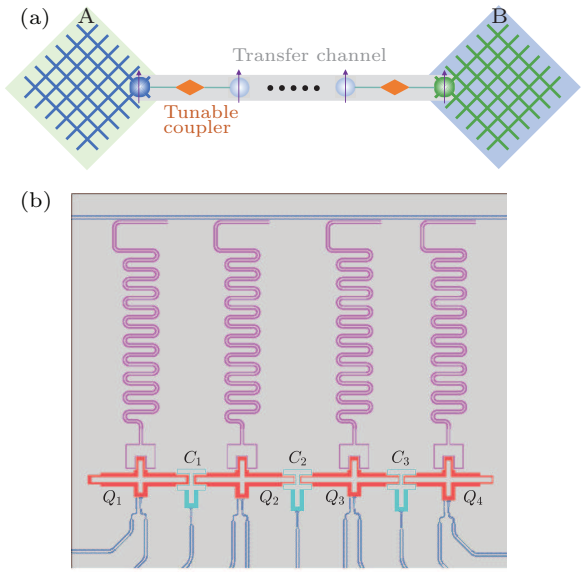


Fig. 1. (a) Two sub-processors A and B are connected with a PST channel. The tunable couplers in the transfer channel can be turned on to allow information flow between A and B, and can also be turned off to ensure independent functioning of the two sub-processors. (b) The layout of our device. Our sample is a four-qubit chain (red, Q_1–Q_4) and each nearest-neighbor two qubits are coupled via a coupler (blue, C_1–C_3). All the qubits and couplers are frequency tunable transmons.

In this work, we utilize this tunable coupler architecture to demonstrate a fast and high-fidelity PST in a chain of four superconducting transmon qubits with tunable couplers in between. With the high on–off ratio of the tunable couplers, the transfer cycle is accomplished efficiently in a single step, and it is as fast as 25 ns, comparable to the shortest duration of a single swap operation in superconducting circuit.[26,27] To realize the exact Hamiltonian required for PST, we employ the differential evolution (DE) algorithm[28] to fine-tune the control parameters and realize nearly PST with a fidelity of 0.986. Simulation and a more detailed error matrix analysis show that this fidelity is mainly limited by the short decoherence time of our sample.

2. Experiment setup and methods

Our experimental device is depicted in Fig. 1(b), where four frequency-tunable transmon qubits (Q_1–Q_4) line up with the tunable couplers (C_1–C_3) sandwiched between each pair of qubits. Each qubit, dispersively coupled to an independent readout resonator, has its own XY and Z control lines; the coupler is only equipped with Z control line. The frequency of the qubit or coupler can be tuned dynamically using ac-bias or statically using dc-bias applied on its Z control line. The effective coupling strength between a pair of adjacent qubits Q_i and Q_{i+1} can be described by[23]

$$g_i = g_{i,i+1} + \frac{g_{i,c_i} g_{i+1,c_i}}{\Delta}, \tag{1}$$

where $\frac{1}{\Delta} = \frac{1}{2}\left(\frac{1}{\omega_i - \omega_{c_i}} + \frac{1}{\omega_{i+1} - \omega_{c_i}}\right)$, ω is the frequency of each element, and $g_{i,j}$ is the direct coupling strength between elements i and j, which is related to their corresponding coupling capacitance and is fixed once designed and fabricated. The system Hamiltonian can be noted as

$$H/\hbar = \Sigma_{i=1}^{4} \frac{\omega_i}{2} \sigma_i^z + \Sigma_{i=1}^{3} g_i \left(\sigma_i^+ + \sigma_i^-\right)\left(\sigma_{i+1}^+ + \sigma_{i+1}^-\right), \tag{2}$$

where $\sigma_i^{z,\pm}$ are the Pauli operators. In experiment, we align the four qubits on resonance so that the σ^z term can be dropped and the effective Hamiltonian in the interaction picture can be simplified as

$$H_{\mathrm{I}}/\hbar = \Sigma_{i=1}^{3} g_i \left(\sigma_i^+ \sigma_{i+1}^- + \sigma_i^- \sigma_{i+1}^+\right). \tag{3}$$

Now the only control parameters are g_i. Furthermore, according to Eq. (1), g_i is solely determined by the frequency of C_i. According to the theory reported in Ref. [18], a quantum state can be transferred perfectly over a qubit chain of any length as long as one can pre-engineer inter-qubit interactions. In addition, in a linear chain of N qubits, PST requires the coupling strengths to follow the function $g_i = g_0\sqrt{i(N-i)}$, where g_0 is a constant. In this condition, when we prepare Q_i in state $|\psi_i\rangle = \alpha|g\rangle + \beta|e\rangle$, and all other qubits are in the ground state $|g\rangle$ ($|e\rangle$ represents the excited state), after a duration $\tau = \pi/2g_0$, Q_{N-i+1} will be in the state $|\psi_{N-i+1}\rangle = |\psi_i\rangle$ (up to a phase factor), and meanwhile all other qubits would turn back to $|g\rangle$. That is, the state from site i can be perfectly transferred to site $N-i+1$.

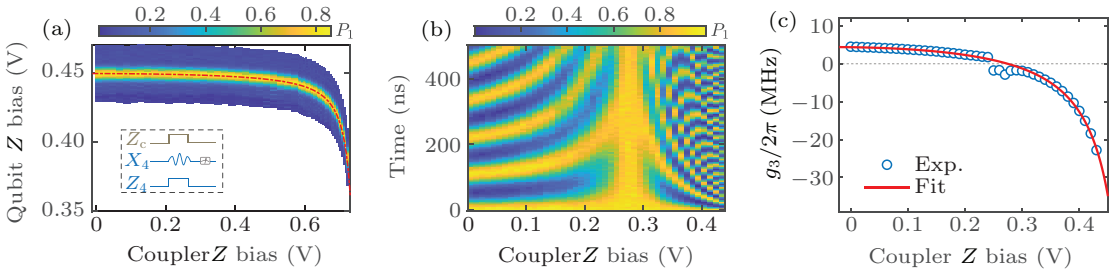


Fig. 2. (a) The relationship of qubit Z bias and coupler Z bias when fixing the qubit frequency at its working point. The insert shows the pules sequences. A π pulse of 500 ns duration with fixed driving frequency is applied on Q_4, when the qubit frequency is correctly compensated, its population would reach the maximum. The red dashed line is the fitted result. (b) Swap spectroscopy between Q_3 and Q_4 when changing the Z bias of C_3, the extracted inter-qubit coupling strength is shown in (c), where we can see that the coupling strength can be effectively turned off and on to more than 30 MHz.

Before showing the tunability of the g_i, we note that the frequency of each qubit is also dependent on the frequency of the nearest-neighboring coupler owing to the strong coupling between them;[29] this will make the tuning process complicated. However, this dependence can be released by compensating the qubit frequency when tuning its adjacent coupler with a pre-calibration experiment. As shown in Fig. 2(a), we fix the drive frequency of Q_4 at the working point while scanning the qubit Z bias and the nearest-neighboring C_3 Z bias simultaneously. The fitted red dashed line in Fig. 2(a) indicates the compensated Z bias of Q_4 for each Z bias of C_3 around Q_4' working point. With this calibration data, the compensation can be done automatically in software, enabling the independent control of qubit frequency and coupler frequency.

The effective inter-qubit coupling strength g_i can be extracted from the swap spectroscopy between Q_i and Q_{i+1}. To demonstrate its tunability, taking g_3 for example, we prepare $|0010\rangle$ by applying a π pulse to Q_3 at its idle point. Then we apply a rapid Z pulse on Q_3 so that $|0010\rangle$ and $|0001\rangle$ are on resonance and meanwhile turning on Q_3–Q_4 coupling by adjusting the Z bias amplitude of C_3. We wait for a variable delay time τ and measure the state population transferred to $|0001\rangle$ as a function of τ and Z bias of C_3. By fitting the oscillation frequencies in Fig. 2(b), we plot the effective coupling strength g_3 as a function of Z bias of C_3, as shown in Fig. 2(c). The inter-qubit coupling strength can be turned off and on to more than 30 MHz. In the same way, we determine g_1 and g_2 as a function of the Z bias of the corresponding coupler, respectively.

Figure 3(a) shows the pulse sequences for the state transfer process. We prepare Q_4 in the excited state while all other qubits stay in the ground state and bring all the qubits and couplers into their working point where the qubits are on resonance and $g_1 : g_2 : g_3 = \sqrt{3} : 2 : \sqrt{3}$. Then we measure the population of each qubit simultaneously as a function of pulse length τ. Flat-top Gaussian pulses are used to suppress the unwanted leakage onto non-computational states. The pulse amplitudes are obtained iteratively using the calibration procedures shown in Figs. 2(a) and 2(b). To further optimize these amplitudes, we use the DE algorithm to minimize the mean squared error between the numerically simulated and experimentally measured trajectories. The final result is shown in Fig. 3(b) for $g_2/(2\pi) = 20$ MHz, where the population of Q_4 (red circle) flows to Q_3, Q_2 and Q_1(blue circle) in turn. The full lines correspond to numerical simulation results. The population of Q_4 is completely transferred to Q_1 at $t = 25$ ns, as expected. Besides, the evolution of population indicates that the transfer continues to go forward and backward as t increases. At $t = 50$ ns, the population of Q_1 is transferred back to Q_4 in turn. As shown below, these repeated transfer cycles offer a straightforward method to benchmark the performance of the process fidelity of QST,[22] such that errors inevitable during state preparation and measurement (SPAM) can be ignored.

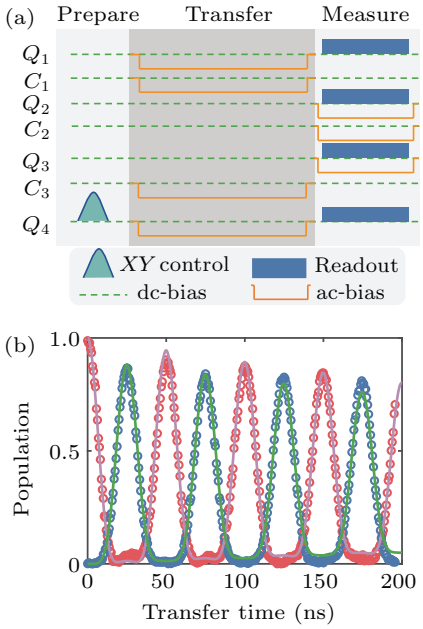


Fig. 3. (a) Pulse sequences for the state transfer process. The XY control pulse is only applied on Q_4 to prepare arbitrary single qubit state. The ac-bias is applied on Q_1, Q_4, C_1, C_3 during the transfer period to bring them to working point, and is also applied on Q_2, Q_3, C_2 during the simultaneous measurement duration. (b) Experimentally measured (circle) and numerically simulated (line) dynamic population flows of Q_4 (red) and Q_1 (blue) during the transfer process.

3. Results

We assess the performance of the PST by performing QPT in this work.[30] Preparing Q_4 in four linear independent initial states $\{|g\rangle, |e\rangle, (|g\rangle + |e\rangle)/\sqrt{2}, (|g\rangle - \mathrm{i}|e\rangle)/\sqrt{2}\}$, we can derive the standard process matrix χ^{exp} that contains a single qubit phase φ accumulated in the quantum state transfer process. We use a χ^{fit} matrix corresponding to a Z rotation operator $U = \begin{bmatrix} 1 & 0 \\ 0 & \mathrm{e}^{\mathrm{i}\varphi} \end{bmatrix}$ to fit the measured χ^{exp}, where the accumulated phase φ is the only fitting parameter. Define the error matrix[31] $\chi^{\mathrm{err}} = V\chi^{\mathrm{exp}}V^{\dagger}$, where $V_{mn} = \mathrm{Tr}(E_m^{\dagger}E_nU^{\dagger})/d$ and E_n are Pauli basis operators, $d = 2$. Then the process fidelity can be defined as $F_{\mathrm{p}} = \mathrm{Tr}(\chi^{\mathrm{err}}\chi^{\mathrm{I}})$, where χ^{I} corresponds to the ideal case with only one non-zero element $\chi^{\mathrm{I}}_{\mathrm{II}} = 1$. Due to the limitation of our control hardware in phase synchronization for different channels, only even times transfers can be investigated in our experiment. By properly controlling the operation time, we perform a series of QPT for different even numbers of transfers. The measured process fidelity is depicted as a function of the number of transfers in Fig. 4(a). Fitting the decay curve in Fig. 4(a) to $F = AP^m + B$, where m is the number of transfers, we get the PST process fidelity $F_{\mathrm{p}} = 0.986$.

Following the error matrix method developed by Korotkov,[31] we can further investigate the error budgets of the PST process. Firstly, the SPAM errors can be deducted, the process matrix without SPAM errors $\chi^{\rm err}_{\rm noSPAM} \approx \chi^{\rm err} - (\chi^{\rm err,I} - \chi^{\rm I})$, where $\chi^{\rm err,I}$ is the measured error matrix of identity gate. Taking the experimental data for transfer times $m = 2$ as an example, as shown in Fig. 4(b), the pure process fidelity without SPAM error $F_{\rm p}(m=2) = 0.965$, from which we estimate the pure process fidelity of single QST $F_{\rm p}(m=1) = \sqrt{F_{\rm p}(m=2)} = 0.982$, agrees well with the fitting result in above. Secondly, by transforming $\chi^{\rm err}_{\rm noSPAM}$ into its diagonal form Λ, as shown in Fig. 4(c), the decoherence error can be extracted,[31,32] $\varepsilon_{\rm dec} = 1 - \Lambda_{\rm II} = 3.06\%$, which indicates that the infidelity of our quantum state transfer process primarily comes from the decoherence error, agreeing well with the numerical result. Moreover, we extract the relaxation time $T_1 = 6.0$ μs and dephasing time $T_2 = 1.5$ μs of the transferred state from the experiment data for the initial state prepared in $|e\rangle$ and $(|g\rangle + |e\rangle)/\sqrt{2}$, respectively. Note that this dephasing time of the transferred state is much longer than the average dephasing time of the four qubits when they are stationary at their working points (~ 0.5 μs), which is consistent with the findings in Ref. [22].

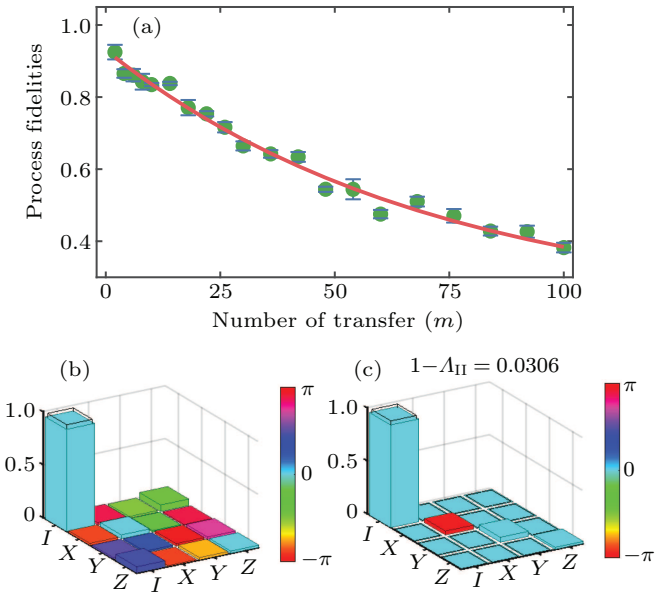


Fig. 4. PST process fidelity. (a) Process fidelity $F_{\rm p}$ decays as transfer number m grows. The error bars are obtained from five repeated experiments representing one standard deviation. Fitting the fidelity data to $F = AP^m + B$ (orange solid line), we get $P = 0.986$, representing a high fidelity QST. (b) Process matrix without SPAM errors $\chi^{\rm err}_{\rm noSPAM}$ for $m = 2$ in the basis of Pauli matrices, with a fidelity $F_{\rm p}(m=2) = 0.965$, from which we estimate the fidelity of single QST $F_{\rm p}(m=1) = \sqrt{F_{\rm p}(m=2)} = 0.982$, agrees well with the fitting result in (a). (c) The diagonalized matrix Λ of $\chi^{\rm err}_{\rm noSPAM}$ for $m = 2$, whose largest eigenvalue $\Lambda_{\rm II}$ is related to the decoherence error, $\varepsilon_{\rm dec} = 1 - \Lambda_{\rm II} = 3.06\%$. The height and color of the bars correspond to the amplitude and phase of the matrix elements, respectively. The transparent outline shows the ideal value.

4. Conclusion

In conclusion, we experimentally realized a fast (25 ns) and high-fidelity (0.986) PST in a chain of four superconducting transmon qubits with tunable coupler architecture. This efficient state transfer is made possible by the large on–off ratio of the tunable coupler. Currently, decoherence is the main error source in PST process. We anticipate that better coherence will further improve PST performance. The PST demonstrated in this work constitutes an important tool for on-chip entanglement generation and distribution. Our technique can also be directly generalized to other different configurations to allow more robust QST,[33–35] and extend to a larger chain or multi-node quantum network,[36] making it a valuable tool for scalable quantum information processing.

Acknowledgements

Project supported by the National Natural Science Foundation of China (Grant Nos. 12034018 and 11625419). This work is partially carried out at the USTC Center for Micro and Nanoscale Research and Fabrication.

References

[1] Preskill J 2018 *Quantum* **2** 79
[2] National Academies of Sciences E and Medicine 2019 *Quantum Computing: Progress and Prospects* (Washington, DC: The National Academies Press) pp. 12–15
[3] He K, Geng X, Huang R, Liu J and Chen W 2021 *Chin. Phys. B* **30** 080304
[4] Arute F, Arya K, Babbush R, *et al.* 2019 *Nature* **574** 505
[5] Wu Y, Bao W S, Cao S, *et al.* 2021 *Phys. Rev. Lett.* **127** 180501
[6] DiVincenzo D P 2000 *Fortschritte der Physik* **48** 771
[7] Cirac J I, Zoller P, Kimble H J and Mabuchi H 1997 *Phys. Rev. Lett.* **78** 3221
[8] Bose S 2003 *Phys. Rev. Lett.* **91** 207901
[9] Romito A, Fazio R and Bruder C 2005 *Phys. Rev. B* **71** 100501
[10] Zhong Y, Chang H S, Bienfait A, Dumur É, Chou M H, Conner C R, Grebel J, Povey R G, Yan H, Schuster D I and Cleland A N 2021 *Nature* **590** 571
[11] Krinner S, Lacroix N, Remm A, Di Paolo A, Genois E, Leroux C, Hellings C, Lazar S, Swiadek F, Herrmann J, Norris G J, Andersen C K, Müller M, Blais A, Eichler C and Wallraff A 2022 *Nature* **605** 669
[12] Zhao Y, Ye Y, Huang H L, *et al.* 2022 *Phys. Rev. Lett.* **129** 030501
[13] Kim Y, Eddins A, Anand S, Wei K X, van den Berg E, Rosenblatt S, Nayfeh H, Wu Y, Zaletel M, Temme K and Kandala A 2023 *Nature* **618** 500
[14] Morvan A, Villalonga B, Mi X, *et al.* 2023 arXiv: 2304.11119
[15] Kurpiers P, Magnard P, Walter T, Royer B, Pechal M, Heinsoo J, Salathé Y, Akin A, Storz S, Besse J C, Gasparinetti S, Blais A and Wallraff A 2018 *Nature* **558** 264
[16] Axline C J, Burkhart L D, Pfaff W, Zhang M, Chou K, Campagne-Ibarcq P, Reinhold P, Frunzio L, Girvin S M, Jiang L, Devoret M H and Schoelkopf R J 2018 *Nat. Phys.* **14** 705
[17] Bienfait A, Satzinger K J, Zhong Y P, Chang H S, Chou M H, Conner C R, Dumur É, Grebel J, Peairs G A, Povey R G and Cleland A N 2019 *Science* **364** 368
[18] Christandl M, Datta N, Ekert A and Landahl A J 2004 *Phys. Rev. Lett.* **92** 187902
[19] Kandel Y P, Qiao H, Fallahi S, Gardner G C, Manfra M J and Nichol J M 2021 *Nat. Commun.* **12** 2156

[20] Zhang J, Long G L, Zhang W, Deng Z, Liu W and Lu Z 2005 *Phys. Rev. A* **72** 012331
[21] Chapman R J, Santandrea M, Huang Z, Corrielli G, Crespi A, Yung M H, Osellame R and Peruzzo A 2016 *Nat. Commun.* **7** 11339
[22] Li X, Ma Y, Han J, Chen T, Xu Y, Cai W, Wang H, Song Y, Xue Z Y, Yin Z Q and Sun L 2018 *Phys. Rev. Appl.* **10** 054009
[23] Yan F, Krantz P, Sung Y, Kjaergaard M, Campbell D L, Orlando T P, Gustavsson S and Oliver W D 2018 *Phys. Rev. Appl.* **10** 054062
[24] Sete E A, Chen A Q, Manenti R, Kulshreshtha S and Poletto S 2021 *Phys. Rev. Appl.* **15** 064063
[25] Goto H 2022 *Phys. Rev. Appl.* **18** 034038
[26] Sung Y, Ding L, Braumüller J, Vepsäläinen A, Kannan B, Kjaergaard M, Greene A, Samach G O, McNally C, Kim D, Melville A, Niedzielski B M, Schwartz M E, Yoder J L, Orlando T P, Gustavsson S and Oliver W D 2021 *Phys. Rev. X* **11** 021058
[27] Huang C, Wang T, Wu F, Ding D, Ye Q, Kong L, Zhang F, Ni X, Song Z, Shi Y, Zhao H H, Deng C and Chen J 2023 *Phys. Rev. Lett.* **130** 070601
[28] Jazzbin *et al.* geatpy: The genetic and evolutionary algorithm toolbox with high performance in python
[29] Zhang C, Wang T L, Guo L L, Yang X Y, Yang X X, Duan P, Jia Z L, Kong W C and Guo G P 2023 *Appl. Phys. Lett.* **122** 024001
[30] Chow J M, Gambetta J M, Tornberg L, Koch J, Bishop L S, Houck A A, Johnson B R, Frunzio L, Girvin S M and Schoelkopf R J 2009 *Phys. Rev. Lett.* **102** 090502
[31] Korotkov A N 2013 arXiv: 1309.6405
[32] Yang X X, Guo L L, Zhang H F, Du L, Zhang C, Tao H R, Chen Y, Duan P, Jia Z L, Kong W C and Guo G P 2023 *Phys. Rev. Appl.* **19** 044076
[33] Mei F, Chen G, Tian L, Zhu S L and Jia S 2018 *Phys. Rev. A* **98** 012331
[34] Liu X Q, Liu J and Xue Z Y 2023 *JETP Lett.* **117** 859
[35] Wang C, Gu X, Chen S and Liu Y X 2023 arXiv: 2305.14529
[36] Humphreys P C, Kalb N, Morits J P J, Schouten R N, Vermeulen R F L, Twitchen D J, Markham M and Hanson R 2018 *Nature* **558** 268